ASIAN JOURNAL OF ORGANIC CHEMISTRY

www.asianjoc.org

Accepted Article

Title: THIOL-ENE COUPLING REACTION FOR FUNCTIONALIZATION OF NON-ACTIVATED ALKENES: AN EXPERIMENTAL STUDY ON THE CHEMISTRY OF THE METHYL OLEATE AMINATION

Authors: Mara L. Polo, David A. Echeverri, Laureana Soria, Victoria A. Vaillard, Gregorio Meira, Santiago E. Vaillard, Luis A. Ríos, and Diana Estenoz

To be cited as: *Asian J. Org. Chem* **2024**, e202400334

Link to VoR: https://doi.org/10.1002/ajoc.202400334

A Journal of

ACES Asian Chemical Editorial Society

WILEY VCH

10.1002/ajoc.202400334

THIOL-ENE COUPLING REACTION FOR FUNCTIONALIZATION OF NON-ACTIVATED ALKENES: AN EXPERIMENTAL STUDY ON THE CHEMISTRY OF THE METHYL OLEATE AMINATION

Mara L. Polo[1,2], David A. Echeverri[3], Laureana Soria[2], Victoria A. Vaillard[2], Gregorio R. Meira, Santiago E. Vaillard[2], Luis A. Ríos[3], Diana A. Estenoz[1,2*]*

[1] Departamento de Ciencia de los Materiales, Facultad de Ingeniería Química, Universidad Nacional del Litoral, Santiago del Estero 2829, (3000) Santa Fe, Argentina.

[2] Instituto de Desarrollo Tecnológico para la Industria Química (INTEC), Universidad Nacional del Litoral and Conicet (UNL-CONICET), Güemes 3450, (3000) Santa Fe, Argentina.

[3] Grupo de Procesos Químicos Industriales, Universidad de Antioquia (UdeA), Calle 70 No. 52-51, (050010) Medellín, Colombia.

Supporting information for this article is provided.

Abstract

This work investigates the functionalization of molecules with non-activated internal double bonds via thiol-ene coupling (TEC) reaction. A comprehensive study of the reaction between cysteamine hydrochloride (CAHC) and methyl oleate (MO) was carried out. A series of reactions were conducted under different operating conditions in order to assess their effect on conversion and selectivity. Different conditions were considered like the type of atmospheres and solvents, a portionwise addition of CAHC, reagents concentrations, and excess of CAHC. Maximum

conversion and selectivity were reached under inert atmosphere, diluted conditions, ethanol as solvent, and the addition of CAHC at the beginning of the reaction with a molar ratio of CAHC/MO of 3/1. This provides an approach for analyzing more complex reaction systems.

1. Introduction

Thiol-ene coupling (TEC) reactions are hydrothiolations that involve the addition of thiol groups onto carbon-carbon double bonds via polar or radical mechanisms [1, 2]. The general mechanisms of TEC reactions involve initiation, propagation, and termination steps [1, 3]. Radical TEC reactions are initiated in the presence of a suitable initiator that decomposes either thermally or by gamma or UV irradiation. TEC reactions were originally considered as "click" because they are conducted under mild experimental conditions, and can exhibit high reaction rates, yields, and selectivities towards a single regio-selective product, with high tolerance to oxygen and water [3-5].

In the last decades, several polymerization processes have employed TEC reactions to obtain polymer precursors or high polymers such as coatings, fibers, hydrogels, films, and adhesives [6], that are applicable in optics, biomedicine, and sensors [4]. However, the "click"-chemistry concept has been controversial in relation to the obtention of polymers or polymer precursors because of: a) the presence of side reactions, such as disulfide formation, homopropagation, or intramolecular formation of five and six-membered cyclic compounds [7]; and b) a varying reactivity that strongly depends on the nature of the double bonds substituents [5]. Thus, in the case of internal double bonds, their lower reactivity compared to terminal bonds requires an excess of thiol, higher initiator concentrations, and longer reaction times, all of which introduce deviations from the "click" concept.

Vegetable oils (VOs) are triglycerides, with a glycerol molecule attached to three fatty acids that may contain one or more double bonds [8]. Due to their structural characteristics, availability, competitive cost, and potential biodegradability [1], several chemical modifications of VOs have been investigated as potential sources of biobased polymer precursors that enable to produce high polymers such as polyamides, polyesters, polyurethanes (PUs), vinyl resins and epoxy resins [8, 9]. In order to obtain such precursors, different synthetic routes are employed that involve hydroformylation/hydrogenation [10-13], transesterification [12, 13], carbonation [14-16], ozonolysis/reduction [12, 13], epoxidation/oxirane ring opening [12, 13, 17, 18], or amidation [12] reactions. The inherent complexity of most of these reactions has spurred an interest in the development of new synthetic routes capable of directly converting VOs into functionalized VOs in a single step, in more economical and environmentally friendly processes. In particular, TEC reactions have been investigated as a simple approach to synthesize polymer precursors from VOs, with functionalities such as: a) alcohol [1, 5, 7, 12, 13, 17, 19-25]; b) cyclic carbonate [26]; c) isocyanate [5]; d) epoxy [5]; e) silane [5]; and f) amine [3, 5, 9, 27-29]. In this last case of the amine VO precursors, all of the mentioned articles have employed cysteamine hydrochloride (CAHC) for the thiol functionality, and with initiators that operated either photochemically [3, 9, 27, 29] or thermally [28].

In this work, we aim at investigating the detailed chemical mechanism of the global TEC reaction between CAHC and methyl oleate (MO) presented in Scheme 1, when carried out at room temperature, in the presence of solvents, with UV irradiation of DMPA, and in an excess of CAHC. Note that instead of a VO, MO is employed as a simple model compound due to its linear structure and its single internal double bond. The main expected product (aminated methyl oleate, AMO) is in principle only a mixture of two regio-isomers, depending on the double bond carbon position where the thiol is added. However, the double bond of MO is not conjugated with the carboxylate

10.1002/ajoc.202400334

group, which decreases their reactivity towards nucleophilic radicals, such as the sulfur-centered radical derived from CAHC. As we shall see from our experiments, higher molar mass contaminants are also obtained.

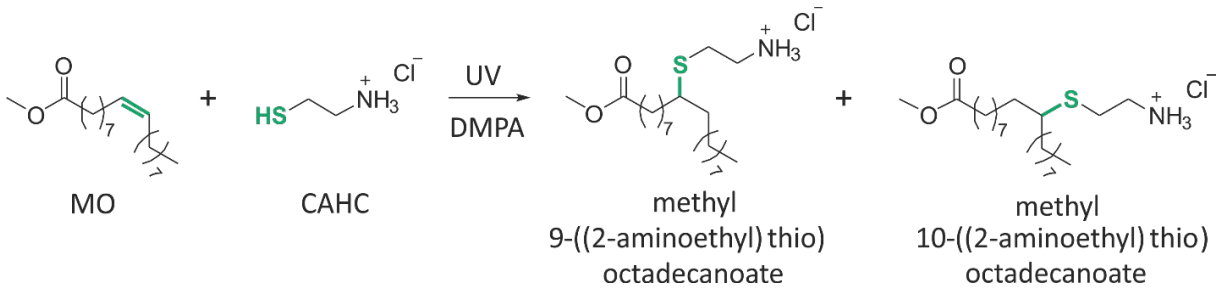

Scheme 1. TEC reaction between MO and CAHC. The main expected product (AMO) is in principle a mixture of two structural isomers: methyl 9-((2-aminoethyl) thio) octadecanate and methyl 10-((2-aminoethyl) thio) octadecanate.

Several investigations were carried out on the reaction kinetics between thiol and compounds derived from VOs that provide an internal ene functionality [30-43] (See Table S1 in the Supporting Information). The articles in Table S1 are classified according to their thiol and ene functionalities, stoichiometry, type of solvent, type of initiation, type of initiator, temperature, and reaction atmosphere. In particular, our work is comparable to the investigations of Chatgilialoglu and co-workers [32, 34] and González-Paz and co-workers [43], in the use of MO as ene functionality, excess of thiol, photochemical initiation, and room reaction temperature.

It has been reported that in reactions with internal double bonds, thiyl radicals catalyze *cis/trans* fatty acids isomerization [30-34, 36, 43]. Chatgilialoglu and co-workers [32] reported the detailed mechanism of Scheme 2 for the UV irradiated reaction between thiols and internal mono-unsaturated fatty acid methyl esters (FAMEs) with excess of thiol. The proposed mechanism involves the following steps: i) generation of thiyl radicals (RS$^{\bullet}$) from a hydrogen atom abstraction

10.1002/ajoc.202400334

by the photoinitiator radical (I•); ii) reversible addition of thiyl radicals (RS•) onto double bonds that generates an intermediate carbon-centered radical that fragments in two directions and renews the thiyl radical (RS•) with generation of the *cis/trans* isomers; iii) transfer of a thiol hydrogen atom (RSH) by the intermediate radical that propagates the reaction, generating the main product and the thiyl radical (RS•); and iv) termination of thiyl radicals (RS•) via combination, generating disulfide as secondary product (RS–SR).

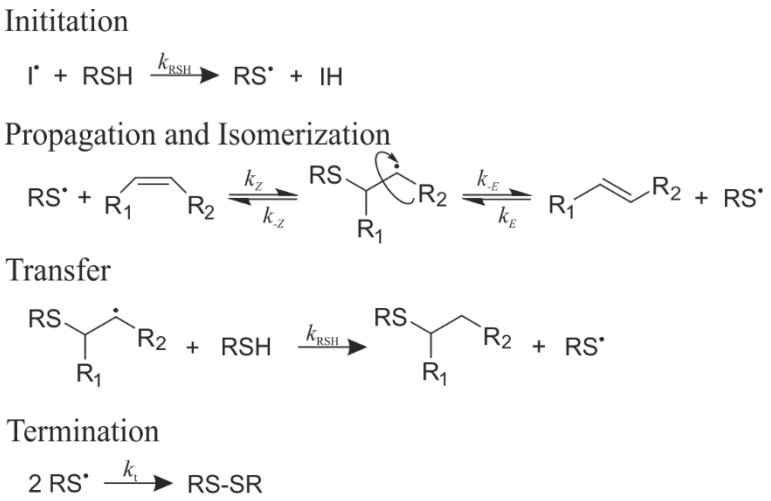

Scheme 2. General mechanism of the TEC reaction between a thiol and an internal mono-unsaturated fatty acid methyl ester proposed by Chatgilaloglu and co-workers [32]. Note that the addition product is generated in the transfer step.

In further investigations, Chatgilialoglu and co-workers [34] reported that inhibition and retardation in the propagation and isomerization steps may occur due to an H-atom abstraction from the allylic methylene groups of FAMEs (see Scheme 3), generating radicals that may later terminate by combination.

10.1002/ajoc.202400334

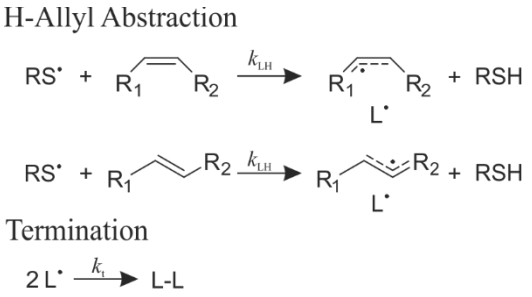

Scheme 3. General mechanism of the H-atom abstraction from the allylic methylene groups of FAMEs and the corresponding termination step, proposed by Chatgilaloglu and co-workers [34].

Regarding photochemical initiation, it can be carried out by: a) direct excitation of the thiol followed by a homolysis of the labile sulfur-hydrogen bond [42]; or b) excitation of cleavable photoinitiators, such as di-*tert*-butyl ketone [32, 34], 1-hydroxy-cyclohexyl-phenyl-ketone (HCPK) [36], and DMPA [43]. In particular, DMPA is a very efficient type I photoinitiator that absorbs UV in the range of 310-390 nm [44]. The free-radical photofragmentation of DMPA is shown in Scheme 4. The carbonyl group absorbs a photon and becomes activated, which leads to a homolytic cleavage of the excited α-carbon bond, yielding methyl benzoate and two radical fragments: a methyl radical and a benzoyl radical [6, 44-46]. Both generated (benzoyl and methyl) radicals could abstract a hydrogen atom from the thiol group, propagating the reaction.

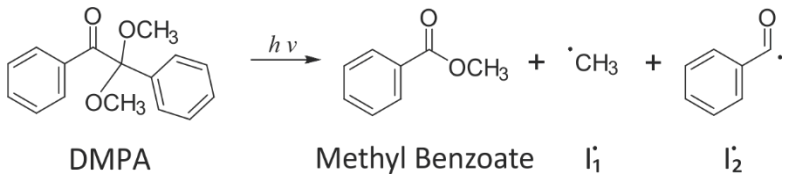

Scheme 4. Fragmentation of DMPA. The carbonyl group absorbs a photon and becomes activated, leading to the cleavage of α-carbon bond into methyl benzoate, and methyl and benzoyl radicals.

This work is the first article of a series that aims to investigate the amine functionalization of internal double bonds *via* TEC reactions between CAHC and MO at room temperature, employing

2,2-dimethoxy 2-phenylacetophenone (DMPA) as photoinitiator, with the final goal of elucidating the chemical kinetics. The aim of this first article is to find the best set of reaction conditions between CAHC and MO to maximize the production of AMO. In the second article, a mathematical model of an extended kinetic mechanism is derived.

In this article, the mentioned reaction is experimentally investigated for analyzing the effects on double bonds conversion and selectivity of: a) the type and total concentration of solvent; and b) the excess of CAHC. Spectroscopic techniques (^{1}H-NMR) are employed for monitoring the reactions. The final product of the best reaction conditions was characterized by: a) spectroscopic techniques (NMR and FTIR); and b) size exclusion chromatography, SEC). In addition to the main reactions, other simpler experiments were carried out to determine: a) the solubility of CAHC; b) the fragmentation of the photoinitiator; c) the effect of dissolved oxygen; d) the effect of not employing a photoinitiator; and e) the initiation of CAHC. As far as we are aware, this is the first article that reports an extended experimental study of the TEC reaction between an amino thiol (CAHC) and an alkene containing an internal double bond (MO).

2. Experimental Work

A series of experiments were carried out to assess the effect of the reaction conditions on conversion and selectivity. The experimental conditions involved variations in: a) the reaction atmospheres (air, inert gas: nitrogen or argon); b) the solvents (a 1:1 mixture of MeOH/EtOH or pure EtOH), c) the reagent concentrations; d) the batch or portionwise additions of thiol; and d) the excess of thiol (molar ratio of CACH/MO/DMPA = 1.5/1/0.1; 2.25/1/0.1; 3/1/0.1; 4.5/1/0.1). Table 1 presents the employed experimental conditions and the main results. The experiments are classified into Series A to D. Series A (Experiments 1 and 2) investigates the dissolution of CAHC.

10.1002/ajoc.202400334

Series B (Experiments 3-5) investigates the fragmentation of the photoinitiator. Series C (Experiments 6-9) investigates the effect of each individual component on the reaction system. Series D involves TEC reactions (Experiments 10-19) and aims at selecting the best conditions for maximizing conversion and selectivity towards thiolated products.

2.1. Materials

Oleic acid technical grade (90 %), CAHC (≥ 98 %), and DMPA were supplied by Sigma Aldrich. Ethanol (EtOH), methanol (MeOH), THF, H_2SO_4, diethyl ether, sodium sulphate, and sodium carbonate (Na_2CO_3) were supplied by Cicarelli (Argentina). Methyl oleate (MO) was obtained by acid catalysis with methanol as solvent (experimental details and MO characterization are provided in the Supporting Information). NMR solvents (deuterated chloroform, $CDCl_3$, deuterated methanol, CD_3OD, and deuterated water, D_2O) were obtained from Deutero GmbH and Laboratorio P.I.A.P. (Argentina), respectively. All the reagents and solvents were used as received, without further purification.

2.2. Characterization Techniques

2.2.1. Series A to C

^{1}H-NMR measurements of simple reactions were performed in $CDCl_3$, CD_3OD or H_2O + D_2O in a Bruker Avance II 300 MHz spectrometer. Coupling constants are given in Hz, and chemical shifts are reported in ppm. Data are reported as follows: chemical shift, multiplicity, coupling constants, and integration. UV-Vis analyses of the photoinitiator fragmentation were performed on a Shimadzu UV-Vis spectrophotometer.

10.1002/ajoc.202400334

Table 1. Experimental Conditions and Main Results: Molar Concentrations of Reagents, Reaction Atmospheres, Employed Solvents, and Conversions and Selectivities at t = 24 h.

Exp.	Molar Ratio	Molar Concentrations (M)			Reaction	Solvent		Results at t = 24 h	
	CAHC/MO/DMPA	CAHC	MO	DMPA	Atmosphere	Type	Volume (mL)	Conversion (x_{DB})	Selectivity (S)
	Series A								
1	—	1.76	—	—	Air	MeOH/EtOH	0.250	—	—
2	—	0.45	—	—	Air	EtOH	0.250	—	—
	Series B								
3	—	—	—	0.001	N_2	MeOH/EtOH	50.0	—	—
4	—	—	—	0.001	N_2	EtOH	50.0	—	—
5	—	—	—	0.130	N_2	CD_3OD	0.6	—	—
	Series C								
6	0.0/1.0/0.1	—	5	0.5	Air	MeOH/EtOH	0.6	—	—
7	0.0/1.0/0.1	—	5	0.5	N_2	MeOH/EtOH	0.6	—	—
8	3.0/1.0/0.0	15	5	—	Ar	EtOH	0.6	—	—
9	1.0/0.0/1.0	0.13	—	0.13	N_2	CD_3OD	0.6	—	—
	Series D								
10	3.0/1.0/0.1	7.84	2.61	0.22	Ar	MeOH/EtOH	1.6	0.36	0.60
11	**3.0/1.0/0.1**	**6.68**	**2.22**	**0.22**	**Ar**	**EtOH**	1.6	**0.95**	**0.90**
12	3.0/1.0/0.1	13.36	4.43	0.44	Ar	EtOH	0.8	0.94	0.73
13	3.0/1.0/0.1	13.36*	4.43	0.44	Ar	EtOH	0.8	0.93	0.76
14	1.5/1.0/0.1	3.34	2.22	0.22	Ar	EtOH	1.6	0.87	0.87
15	2.25/1.0/0.1	5.01	2.22	0.22	Ar	EtOH	1.6	0.94	0.84
16	4.5/1.0/0.1	10.08	2.22	0.22	Ar	EtOH	1.6	0.95	0.82
17	1.5/1.0/0.1	6.68	4.43	0.44	Ar	EtOH	0.8	0.90	0.71
18	2.25/1.0/0.1	10.02	4.43	0.44	Ar	EtOH	0.8	1.00	0.85
19	4.5/1.0/0.1	20.10	4.43	0.44	Ar	EtOH	0.8	0.88	0.84

*CAHC was added in two fractions: 6.68 M at t = 0 h, and 6.68 M at t = 4 h.

2.2.2. Series D

The ^{1}H-NMR spectra of the TEC reactions were obtained using a Bruker Avance III (600 MHz) spectrophotometer in $CDCl_3$ as solvent. The spectra were processed using the ACD Processor/NMR software. Reagents and products were analyzed by FTIR using a Prestige 21 Shimadzu IR spectrophotometer with an accessory of attenuated total reflectance (ATR). The turbidity of the reaction systems was indirectly determined by measuring the absorbances at 600 nm. Aqueous suspensions of $BaSO_4$ were standards for obtaining a calibration curve of turbidity *vs* absorbance (see Figure S2, Supporting Information). The turbidity of the $BaSO_4$ standards (20, 100, 300, 500, and 700 ppm) was measured in a portable turbidimeter Hach 2100q. The UV-Vis analyses of the $BaSO_4$ standards and the reaction samples were performed on a Shimadzu UV-Vis spectrophotometer. The SEC analyses were performed on a chromatograph equipped with an HPLC Waters pump model 515, a Rheodyne 7725i injector, a set of 10 μm PLgel fractionation columns, and a Waters 2412 differential refractometer. The eluent was THF at 1 mL/min, and the chromatographic system was operated at room temperature.

2.3. Main Experiments

2.3.1. Series A

The solubilities of CAHC in MeOH/EtOH and EtOH were determined in Experiments 1 and 2 by the shake flask method at 25°C. Briefly, the CAHC solution was prepared by adding an excess of salt to the solvent, with a stirring rate of 50 rpm for 24 h. The concentrations of CAHC and cystamine dihydrochloride (formed in solution in the presence of O_2) [47] were calculated by ^{1}H-NMR employing D_2O as solvent and using sodium acetate as the internal standard, through:

$$mmol\ X = \frac{(A_X/2)\times mmol_{Ac}}{(A_{Ac}/3)} \quad [1]$$

where A_X is the relative area of the peak corresponding to –CH_2– groups of CAHC or cystamine dihydrochloride, and A_{Ac} is the relative area of the peak corresponding to –CH_3 group of sodium acetate.

2.3.2. Series B

The fragmentation of DMPA in both MeOH/EtOH and EtOH was investigated in: a) Experiments 3 and 4 by UV-Vis spectroscopy (Table 1); and b) Experiment 5 by ^{1}H-NMR employing CD_3OD. In Experiments 3 and 4, diluted solutions (0.001 M) of DMPA in MeOH/EtOH or EtOH were prepared and transferred to 1 cm^3 quartz cuvettes under an inert atmosphere and were then irradiated at room temperature for fixed times. The inert atmospheres were obtained by bubbling the samples with N_2 for 30 min. The cuvettes were irradiated by a set of 4 lamps of 8 W each, and the distance between the lamps and the cuvettes was 5 cm. The emission spectrum was measured with a fiber optic spectrometer, resulting in a range between 300 and 400 nm, with a maximum emission of 368 nm and an irradiance of 12.5 mW/cm^2. The UV absorbance was measured in the range 300-400 nm. The fragmentation of DMPA was monitored by the changes in the absorbance at 338 nm (*i.e.* the wavelength of the maximum absorption), until no further significant change in the absorption spectrum. The absorbance background was subtracted from each sample by employing a blank sample of only solvent. The range of concentrations employed (0.5-2.3 mM) obeys the Beer-Lambert law for both solvents (see Figure S1, Supporting Information). In Experiment 5, DMPA was dissolved in CD_3OD and magnetically stirred in a Schlenk reactor. Once the mixture was homogenous, the solution was transferred to a screw-cap NMR tube and irradiated at room temperature under a nitrogen atmosphere. Irradiation was performed with only one of the 8 W-lamps previously

described, which was located at a distance of 19 mm from the reaction center. *In situ* NMR measurements were carried out to monitor the time evolution of DMPA and methyl benzoate.

2.3.3. Series C

The effect of the individual reaction components on the system was investigated by ^{1}H-NMR in Experiments 6-9 (Table 1). Experiments 6-8 were carried out at room temperature in Schlenk reactors with magnetic stirring and under air or inert atmosphere. The reactors were irradiated for 6 h by the same set of lamps as Experiments 1 and 2, maintaining the same distance between lamps and reactors. Then, the reaction mixtures were added to 50 mL of a sodium carbonate solution, and extracted with ethyl ether (3 × 50 mL). The combined organic extracts were washed with water (50 mL), dried over anhydrous sodium sulphate and filtered, and the solvent was eliminated under vacuum at room temperature. The dry organic extracts were analyzed by ^{1}H-NMR in $CDCl_3$. In Experiment 9, reagents were first dissolved in CD_3OD and magnetically stirred in a Schlenk reactor. Once the mixture was homogenous, the solution was transferred to a screw-cap NMR tube and irradiated at room temperature under a nitrogen atmosphere. Irradiation was performed with an 8 W-lamp located at a distance of 19 mm from the reaction center. *In situ* ^{1}H-NMR measurements were carried out at different times to monitor the evolution of CAHC initiation. The irradiation of CAHC in the presence of DMPA generates cystamine dihydrochloride, a disulfide by-product derived by termination between two thiyl radicals.

2.3.4. Series D

The TEC reactions in Experiments 10-19 (Series D) were carried out to investigate the effects of the reagents concentration and the excess of CAHC on conversion and selectivity. The reagents concentrations were modified by varying the solvent volume (1.6 and 0.8 ml), and the excess of CAHC was evaluated by varying the reagents molar ratio (CAHC/MO/DMPA =

1.5/1.0/0.1, 2.25/1.0/0.1, 3.0/1.0/0.1, and 4.0/1.0/0.1). All the reactions were carried out at room temperature in batch reactors and under an inert atmosphere. Pyrex glass tubes (16 mm outside diameter, 13 mm inside diameter) stirred by a magnetic stir bar in a vertical position at 300-500 rpm were irradiated by a single 9 W UV lamp. In Series D, the UV irradiation was lower than in Series C due to the experimental setup. This should not affect the reaction mechanism and the distribution of products but affects the kinetics [48]. The emission spectrum consisted of > 99.99% UVA1 radiation (340-400 nm) and < 0.01% UVA2 (315-340 nm), with maximum emission at 365 nm. The solvents were methanol:ethanol or pure ethanol. In a typical experiment, CAHC was mixed with the solvent in a Pyrex glass tube, and the mixture was stirred at room temperature for 10 min. DMPA was dissolved in MO by stirring in a beaker and this solution was then added to the CAHC solvent mixture. The UV-irradiated reactions were carried out under argon atmosphere for 24 h. During the reactions, samples were withdrawn at 2, 4, 7, and 24 h to determine double bond *cis/trans* isomerization, conversion, and selectivity by ^{1}H-NMR. Each sample was transferred to a separation funnel, where a saturated Na_2CO_3 solution was added. The mixture was shaken and the phases were settled and separated. The organic phase was washed with deionized water until neutral pH. Afterwards, the organic phase was dissolved in diethyl ether and dried over anhydrous sodium sulphate. Finally, the solvent was evaporated in a rotary evaporator at 40 °C.

The organic extracts were characterized by ^{1}H-NMR for determining double bond *cis/trans* isomerization, conversion, and selectivity. The double bond *cis/trans* isomerization was estimated by comparison of the relative area of the peaks at 5.34 and 5.39 ppm, that respectively correspond to the *cis* and *trans* configurations. The conversion of MO double bounds (x_{DB}) and the selectivity (S) were calculated through:

$$x_{DB}\ (\%) = \frac{A_{CH=CH|MO} - \sum(A_{CH=CH|Reaction\ Mixture})}{A_{CH=CH|MO}} \times 100 \qquad (2)$$

$$S\ (\%) = \frac{A_{CH2-NH2}}{A_{CH=CH|MO} - \sum(A_{CH=CH|Reaction\ Mixture})} \times 100 \quad (3)$$

where $A_{CH=CH}$ corresponds to the normalized areas of vinyl protons in ^{1}H-NMR spectra at 5.34-5.39 ppm; and $A_{CH2-NH2}$ corresponds to the normalized area of methylene protons bonded to amine groups at 2.95 ppm. Note that the selectivity refers to the thiolated products, and this includes AMO and other compounds obtained by termination steps. The peaks were normalized taking as reference the integral of $–CH_3$ protons of MO at 0.85-0.91 ppm (corresponding to 3 protons). In addition, the effect of turbidity on the reaction system was investigated in Experiments 13 and 17 through UV-Vis spectroscopy, with a turbidity *vs* UV-Vis absorption calibration curve.

To further study the nature and composition of the radical addition reaction, the mixture of AMO regio-isomers in the best reaction conditions (Experiment 11) was isolated by column chromatography (silica gel), employing elution gradients (hexane:ethyl acetate = 98:2 to 50:50, ethyl acetate:methanol 10:1 in 31% isolated yield); and characterized by ^{1}H-NMR, ^{13}C-NMR, and FTIR. For structural elucidation, complementary 2D experiments were performed. Their data and spectra are provided in the Supporting Information (Figures S3-S9). Finally, the product distributions in the reaction of Experiment 13 and the mixture of the corresponding AMO isomers after purification were analyzed by SEC, and compared with MO.

^{1}H-NMR [300 MHz, $CDCl_3$] δ (ppm): 0.85-0.90 (*m*, 3H, –***CH₃*** terminal), 1.12-1.43 (*m*, 22H, –***CH₂***– from fatty chain), 1.43-1.68 (*m*, 6H, –***CH₂***– from fatty chain); 2.30 (*t*, *J* = 7.5, 2H, –***CH₂***–C(O)OCH_3), 2.51-2.61 (*m*, 1H,

–CH_2–***CH***($S(CH_2)_2NH_2$)–CH_2–), 2.62-2.69 (*m*, 2H, –S–***CH_2***–CH_2–NH_2), 2.95 (*t*, *J*= 6.4, 2H, –S–CH_2–***CH_2***–NH_2); 3.04 (*bs*, 2H, –***NH_2***), 3.66 (*s*, 3H, –C(O)O–***CH_3***).

^{13}C-NMR [70 MHz, $CDCl_3$] δ (ppm): 14.1 (–CH_3), 22.6 (–CH_2), 24.9 (–CH_2), 26.6 (–CH_2), 26.7 (–CH_2; 2C), 29.1-29.6 (–CH_2, 11 C), 31.8(–CH_2), 32.8(–CH_2), 34.0 (–CH_2, 2C), 34.8 (–CH_2, 3C), 41.0(–CH_2), 45.9 (–CH), 51.4 (–CH_3), 174.2 (–CO).

3. Results and Discussion

3.1. Series A

Experiments 1 and 2 (Table 1) were carried out in order to study the CAHC dissolution kinetics in methanol:ethanol and in ethanol. Figure 1 presents the time evolution of dissolved CAHC. As observed, a higher dissolution rate was obtained when methanol:ethanol was employed. As seen in Figure 1, the final solubilities were 1.76 mmol CAHC/mL in methanol:ethanol and 0.45 mmol CAHC/mL in ethanol.

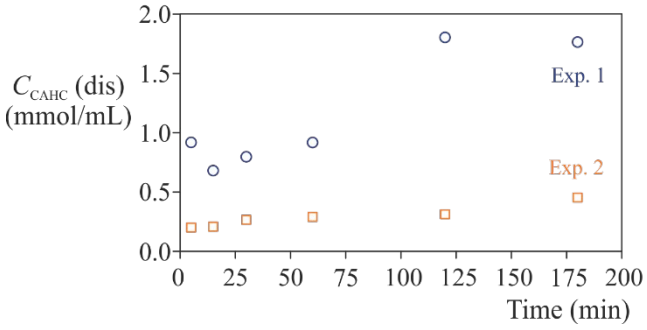

Figure 1. CAHC Dissolution: Concentration of dissolved CAHC as a function of time in methanol:ethanol (Experiment 1) and in ethanol (Experiment 2).

3.2. Series B

Figure 2 presents the measurements involving DMPA fragmentation. Experiments 3 and 4 (Table 1) were monitored by UV-Vis spectroscopy to study the effect of the solvent on the photoinitiator fragmentation. Figure 2a presents the evolution of the absorbance *vs* irradiation

time for a diluted solution of DMPA in both solvents. A higher fragmentation rate was observed for DMPA in ethanol compared with DMPA in methanol:ethanol. In addition, Experiment 5 (Table 1) was carried out to investigate the fragmentation kinetics of DMPA. Figure 2b presents the time evolution of DMPA and the main fragmentation product (see Scheme 2): methyl benzoate. Note that the decrease in the concentration of DMPA is equal to the increase in the concentration of methyl benzoate, in concordance with Fisher and co-workers [45] and Degirmenci [46].

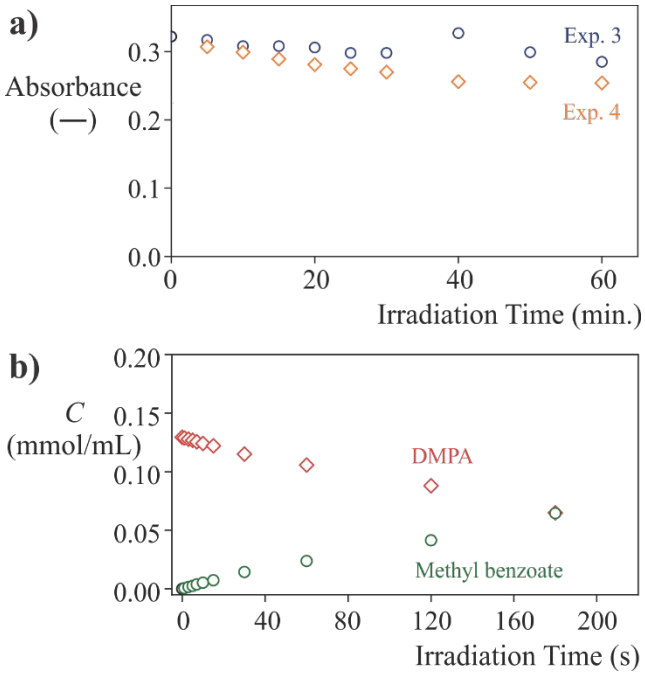

Figure 2. DMPA Fragmentation. a) Absorbance as a function of irradiation time for a diluted solution of DMPA in methanol:ethanol (Experiment 3) and in ethanol (Experiment 4). b) Time evolution of DMPA and methyl benzoate concentrations obtained by ^{1}H-NMR in CD_3OD (Experiment 5).

3.3. Series C

The effect of the reaction atmosphere on the reaction was studied in Experiments 6 and 7 (Table 1), by irradiating MO in the presence of DMPA under air or nitrogen. Figure 3 presents

the ^{1}H-NMR spectra of MO and the organic extracts of both experiments, together with the assignment of signals. As expected, the peak at 5.35 ppm (*f*), corresponding to MO double bonds, reveals that no isomerization of MO (*cis* configuration) into methyl elaidate (*trans* configuration) had occurred. These results indicate that *cis/trans* isomerization does not occur when thiyl radicals are not present, as reported in the literature [34]. In the presence of air (Experiment 6), two new peaks appear at 3.94 and 3.24 ppm. This could suggest that MO is oxidized through a free radical mechanism, generating peroxide groups [39, 42, 47]. However, under inert atmosphere (Experiment 7), no differences between non-irradiated MO and irradiated MO spectra are observed. Therefore, the subsequent reactions were carried out under inert atmosphere.

10.1002/ajoc.202400334

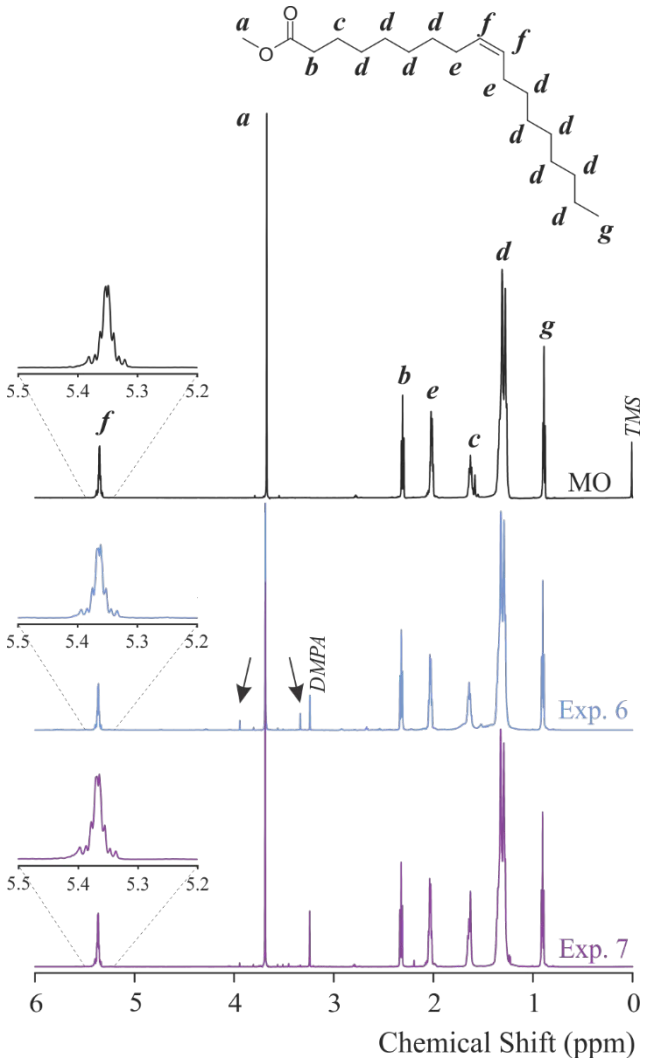

Figure 3. Effect of reaction atmosphere: ^{1}H-NMR spectra of MO and organic extracts of reactions between MO and DMPA under air (Experiment 6) or inert atmosphere (Experiment 7).

The effect of the absence of the photoinitiator was considered in Experiment 8 (Table 1), where the reaction between CAHC and MO was carried out in ethanol. Figure 4 presents the ^{1}H-NMR spectra of MO and the organic extract of Experiment 8, together with the assignment of main signals. Note that the signals at 5.3-5.5 ppm in Experiment 8 showed isomerization of double bonds, suggesting the generation of thiyl radicals and their reversible addition onto the double bonds. In addition, the broad peaks observed at 0.8-2.3 ppm in Experiment 8 could be related to the formation of non-thiolated products with a structure similar to MO.

10.1002/ajoc.202400334

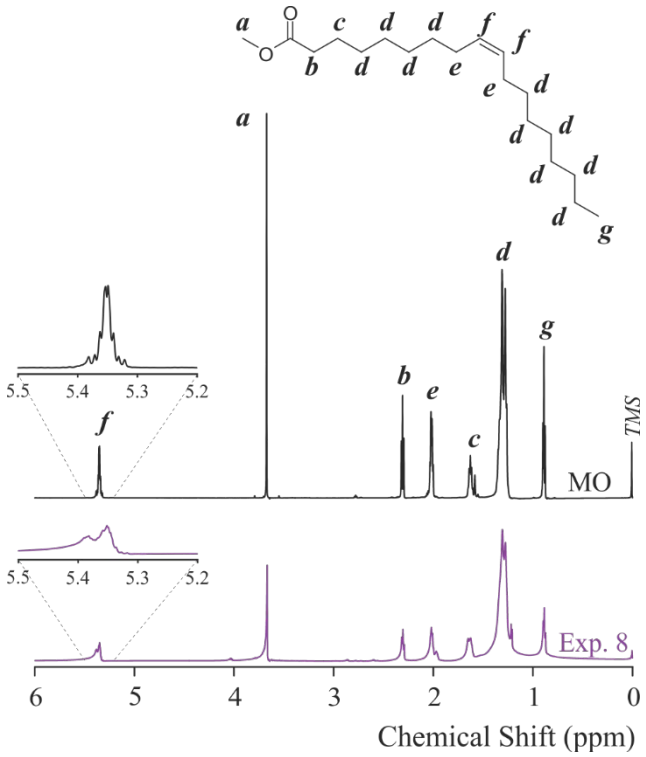

Figure 4. Effect of the absence of the photoinitiator: ^{1}H-NMR spectra of MO and organic extract of the reaction between CAHC and MO without photoinitiator and in ethanol (Experiment 8).

The initiation of CAHC with equimolar amounts of DMPA as photoinitiator was investigated in Experiment 9 (Table 1), and Figure 5 shows the time evolution of CAHC and cystamine hydrochloride concentrations determined from the ^{1}H-NMR spectra. As expected, cystamine disulfide is the single termination product from the UV-Vis initiation of CAHC, and its concentration is one-half of the CAHC concentration.

10.1002/ajoc.202400334

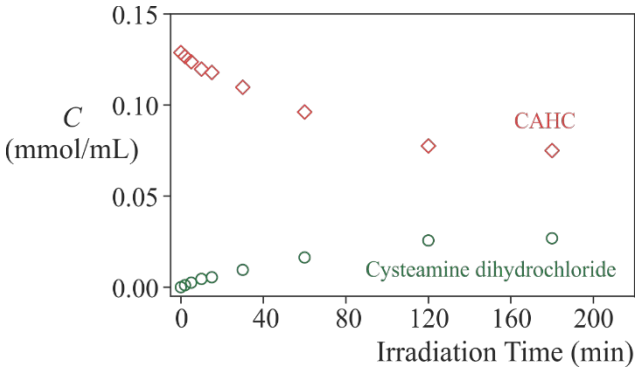

Figure 5. Initiation of CAHC: Time evolution of CAHC and cysteamine hydrochloride concentrations obtained by ^{1}H-NMR in CD_3OD (Experiment 9).

3.4. Series D

The main results of Experiments 10-19 are shown in Figures 6 and 7. The organic extracts of all these experiments were characterized by ^{1}H-NMR. As an example, Figure 6 shows the ^{1}H-NMR spectra of MO and of the organic extracts in Experiment 11 (Table 1) at different reaction times (t = 4, 7, and 24 h). The main evidences of thiol-ene addition were: a) the disappearance of vinyl protons at 5.35 ppm from MO (*f*); b) the formation of methylene (–CH_2–) protons linked to the amino (–NH_2) group at 2.8-2.94 ppm (*k*); and c) the presence of methine (–CH–) and methylene protons bonded to the thiol (–SH) group at 2.5-2.7 ppm (*h*, *j*). The signals at 5.2-5.5 ppm in Figure 6 are expanded to appreciate the *cis/trans* isomerization of the MO double bond during the thiol-ene addition. The MO double bond appears around 5.35 ppm (*f*) and corresponds to the *cis* configuration. At 4 h of reaction, 34% of the double bonds were consumed; but now most of the remaining double bonds were in the *trans* configuration. *Cis/trans* isomerization increased progressively with C=C conversion along the reaction. Isomerization has been reported during thiol-ene addition, and it consists of the reversible addition of thiyl radical to the double bond to produce a *trans* configuration that is thermodynamically more stable than the *cis* [49, 50].

10.1002/ajoc.202400334

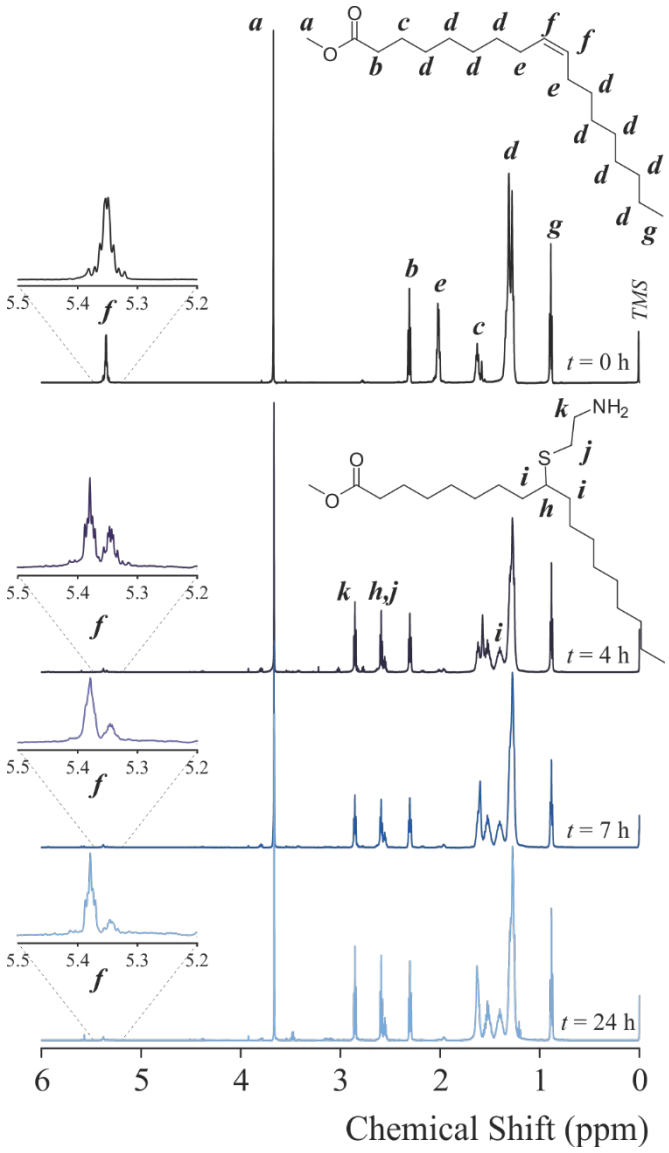

Figure 6. ^{1}H-NMR spectra of MO and organic extracts of samples taken along Experiment 11, and peaks assignment.

Experiments 10-19 employed CAHC concentrations above the solubility limits. For this reason, the effect of the turbidity on the reaction system was studied for the initial reaction mixtures at the following conditions: molar ratio of CAHC/MO/DMPA = 3.0/1.0/0.1, ethanol as solvent, inert atmosphere, and both lower and higher reagents concentrations (Experiments 11 and 12, respectively). Figure S2 (Supporting Information) shows the turbidity *vs* absorbance calibration curve using $BaSO_4$ standards. The initial mixtures for Experiments 11 and 12 were

measured at 600 nm, and the turbidity values were calculated employing a calibration curve, yielding approximately 1160 and 2010 NTU, respectively.

The effect of the solvent, portionwise additions of thiol, concentrations of reagents, and excess of CAHC were investigated in Experiments 10-19 (Table 1) for the TEC reactions between CAHC and MO using DMPA as photoinitiator, and are shown in Table 1 and Figure 7. Figure 7 presents the time evolution of the conversion of double bonds and selectivity.

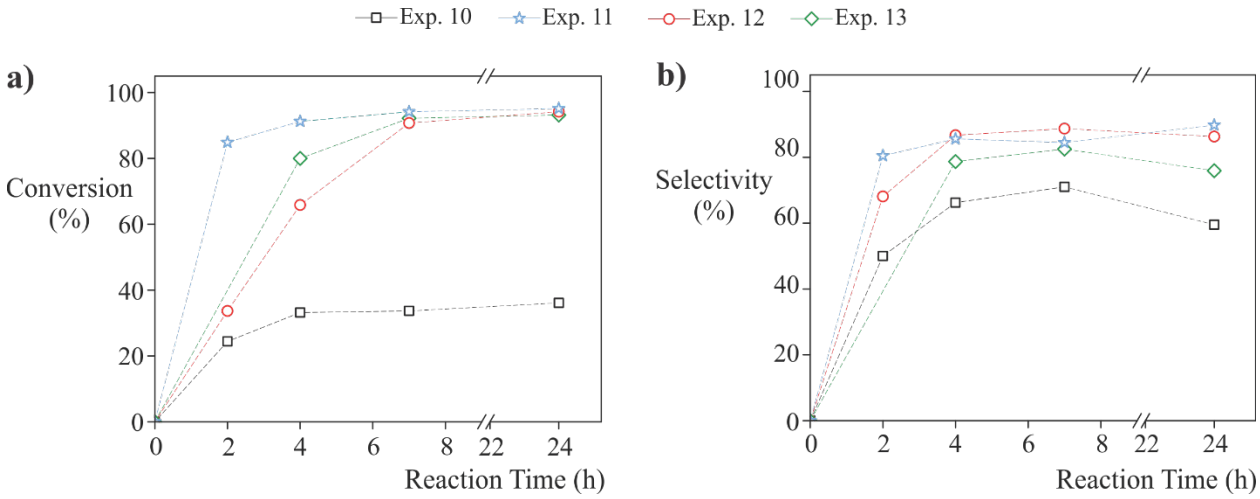

Figure 7. Experiments 10-13: The time evolution of the conversion of the double bonds (a), and the selectivity (b), for a CAHC/MO/DMPA ratio of 3.0/1.0/0.1, and different solvents and reagents concentrations. Experiment 10 (black squares): MeOH/EtOH as solvent, and lower concentration of reagents. Experiment 11 (blue stars): EtOH as solvent, and lower concentration of reagents. Experiment 12 (red circles): EtOH as solvent, and higher concentration of reagents. Experiment 13 (green rhombus): EtOH as solvent, a higher concentration of reagents, and addition of CAHC in two fractions.

Associated with the conversion of double bonds and with selectivity, the effect of the solvent can be analyzed by comparing the reaction between CAHC and MO in methanol:ethanol (Experiment 10) and in ethanol (Experiment 11). Conversion was lower for the reaction carried

out in methanol:ethanol (Experiment 10), in accordance with the fragmentation kinetics of the DMPA photoinitiator, and also probably due to solvent effects.

The effect of portionwise additions of CAHC was analyzed by comparing the reaction between MO and CAHC with a single addition of CAHC at the beginning of the reaction (Experiment 12) and with two additions (Experiment 13); with the first addition at the beginning of the reaction and the second addition after 4 h of reaction. At short reaction times, higher conversions were achieved when CAHC was added in two steps (Experiment 13); but at higher reaction times, similar conversions of around 95% and selectivity of around 74% were obtained in both experiments. These results could be attributed to a lower turbidity generated by a lower quantity of CAHC at the beginning of the reaction (Experiment 13), thus indicating that a lower amount of suspended CAHC increases the fragmentation of the photoinitiator. However, the initial selectivity increased when all the CAHC was added at the beginning of the reaction (Experiment 12). This behavior could be related to the double bond/thiol ratio, which is lower for Experiment 13 at the beginning of the reaction (CAHC/MO/DMPA = 1.5/1/0.1 at t = 0 h), implying that by-products have a greater probability of being generated, thus decreasing selectivity.

The effect of reagents concentration (*i.e.* amount of solvent) was investigated by comparing the reaction between CAHC and MO at lower concentrations (Experiment 11) and higher concentrations (Experiment 12). Note that a lower concentration increases conversion at lower reaction times, due to systems turbidity. In addition, in Experiment 12, the selectivity decreased at long reaction times, probably indicating that the addition of thiyl radicals onto double bonds becomes important.

Finally, the effect of the excess of CAHC at high (Experiments 11, and 14-16) and low (Experiments 12, and 17-19) solvent content was investigated. The values of conversion and

selectivity at the end of the reactions (t = 24 h) are presented in the last columns of Table 1. Note that the CAHC concentrations are over the solubility in all experiments, and for this reason, no significant effect on conversion or selectivity is measured both for diluted and concentrated systems. In addition, the results reveal that the system turbidity does not affect the conversion and selectivity at the end of the reaction. Regarding experiments with the same reagents molar ratio but different amounts of solvent, similar conversions were obtained. However, higher selectivities were obtained for experiments with higher amounts of solvent, because of a lower probability of secondary reactions associated with the lower concentration of double bonds.

The results of the TEC reactions (Experiments 10-19) show that higher conversions and selectivities are obtained when the reactions are carried out in ethanol and under inert atmosphere, with lower concentrations of reagents (higher amounts of solvent) and when adding all CAHC at the beginning of the reaction (Experiment 11 and 14-16).

The *trans/cis* ratio was calculated for Experiments 10-13. In all cases, it resulted in 4.2 ± 0.4, *i.e.* close to the *trans/cis* ratio of 4.3 in methanol reported by Sprinz and co-workers [51] and of 5.15 in *tert*-butanol reported by Chatgilialoglu and co-workers [32, 34]. These results imply that equilibrium was reached between *trans* and *cis* configurations for these experiments, and that *trans* configuration reacts faster than the *cis*, as previously reported by Claudino and co-workers [36].

For providing further spectroscopic and chromatographic characterization, the reaction mixture corresponding to the conditions of Experiment 11 (in bold in Table 1) was purified by silica gel column chromatography, and analyzed by FTIR and SEC (Figure 8). After purification, a fraction containing only a mixture of both expected addition products was obtained. Figure 8a compares the FTIR spectra of the purified regio-isomers mixture with the corresponding

spectra of CAHC and MO reagents. The most relevant information obtained from these spectra is the disappearance of the C=C stretching band in *cis* configuration at 3007 cm^{-1} corresponding to MO. In addition, evidence of CAHC addition to MO are the new N–H stretching and N–H bending bands at 3290 cm^{-1}, and at 1642 and 1543 cm^{-1}, respectively, as well as the new C-S stretching vibration at 692 cm^{-1}.

Figure 8b shows the SEC chromatograms of the regio-isomers mixture product after purification obtained from the reaction between MO and CAHC at the conditions of Experiment 11, with the corresponding MO reagent. The chromatogram corresponding to MO presents a main peak at 33.0 mL corresponding to MO, and a secondary peak at 31.1 mL, that could be related to impurities. Along the reaction, the peak corresponding to MO is reduced, and a multimodal molar mass distribution (MMD) appears, with at least three different compounds, with maxima at around 29.8, 30.8, and 32.6 mL. The presence of a multipeak distribution could indicate that the product is a mixture of both regio-isomers of AMO (at 32.6 mL) with other by-products such as higher molar mass oligomers generated by homopropagation and termination reactions.

10.1002/ajoc.202400334

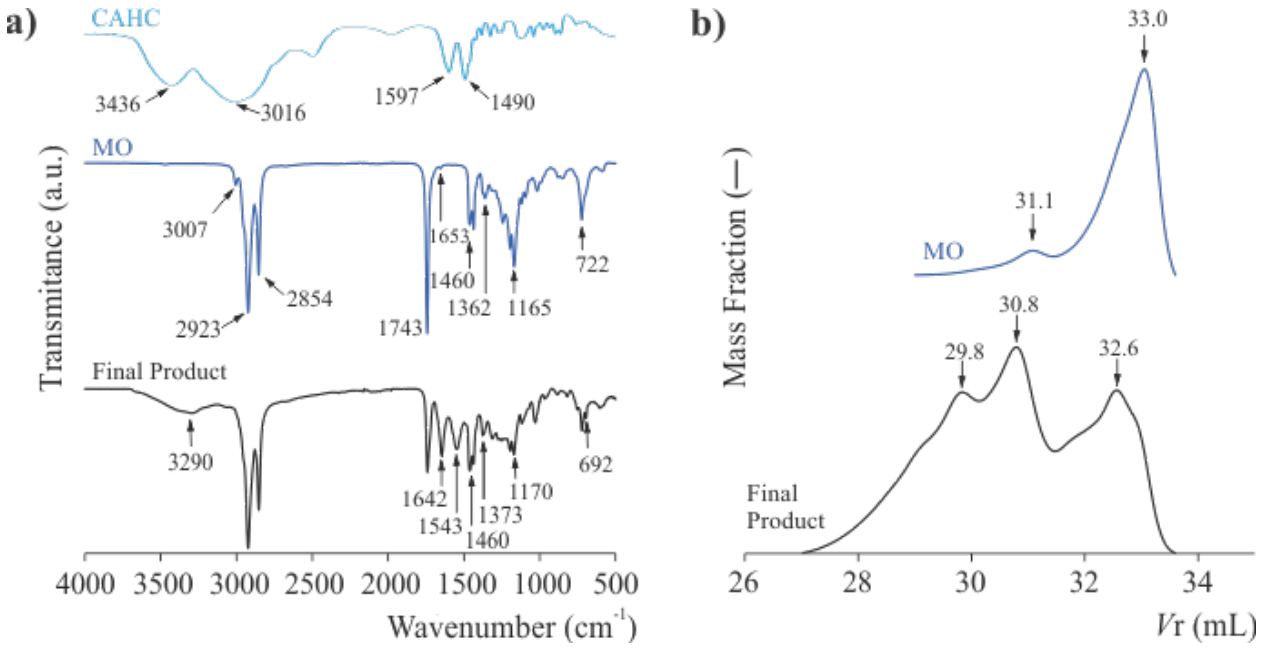

Figure 8. Spectroscopic and chromatographic characterization of the final isolated product mixture obtained from the reaction between MO and CAHC at the conditions of Experiment 11: a) FTIR spectra; and b) SEC chromatograms.

4. Conclusions

The amine functionalization of MO with CAHC *via* TEC reaction was experimentally investigated under different experimental conditions, such as reaction atmosphere (air and inert gas), type of solvents (methanol:ethanol or ethanol), the addition of CAHC in one or two steps, reagents concentrations (amount of solvent), and excess of CAHC. High conversions and selectivities were obtained under conditions of inert atmosphere, diluted conditions, using ethanol as solvent, and adding the CAHC all at once at the beginning of the reaction.

The results of this study suggest that the reaction involves a complex mechanism, that possibly arises from the low reactivity of the internal double bonds. In particular, the homopropagation of intermediate radicals and corresponding termination reactions could be the reason for the relatively important higher molar mass fractions, as were measured by SEC for the purified product of Experiment 11, corresponding to one of the best reaction conditions.

In a future work, and based on the experimental results of Series A to D, a reaction mechanism will be proposed for the TEC reaction between CAHC and MO, which considers the photoinitiator fragmentation, thiol initiation, isomerization of double bonds, homopropagation of carbon-centered radicals, generation of addition products, and termination reactions steps that produce different thiolated and non-thiolated products. This mechanism will include the homopropagation and corresponding termination reactions in order to obtain the observed products. In addition, a mathematical model will be developed based on the proposed mechanism, that will enable to predict the evolution of reagents, radicals, and products over time. To determine the involved kinetic constants, the model will be adjusted to the experimental measurements obtained in this work for the best conditions. The final aim of the model is to optimize the system parameters (reagents molar ratio, amount of solvent) to obtain higher conversions and selectivities.

Supporting Information

Additional experimental details regarding the synthesis of methyl oleate, DMPA concentrations obtained by UV-Vis measurements, turbidity measurements, and NMR spectra of the final product (^{1}H-NMR, ^{13}C-NMR, DEPT-35 ^{13}C-NMR, ^{1}H-^{1}H COSY, ^{1}H-^{13}C-HSQC, ^{1}H-^{13}C-HMBC) are provided in the Supporting Information (PDF).

Acknowledgments

The authors wish to acknowledge financial support from the Universidad Nacional del Litoral (grant Nº CAI+D 2020 50620190100093LI), CONICET (grant Nº PIP 2020 112-202001-00947-CO), and FonCyT (grant Nº PICT 2021 00674). Also, the authors gratefully acknowledge the financial support provided by the Ministry of Science, Technology, and Innovation of Colombia (Minciencias) within the call No. 914-2022 (contract No. 80740-098-

2022). Furthermore, the authors also extend their sincere gratitude to Laboratorio P.I.A.P. for kindly providing deuterated water.

Keywords

Thiol-ene coupling, click chemistry, ene reaction, isomerization, photochemistry.

REFERENCES

[1] Alagi, P., Choi, Y.J., Seog, J., Hong, S.C. *Ind. Crops Prod.*, 2016, **87**, 78-88. DOI: 10.1016/j.indcrop.2016.04.027.

[2] Lowe, A. B. *Polym. Chem.*, 2010, **1**(1), 17-36. DOI: 10.1039/B9PY00216B.

[3] Stemmelen, M., Pessel, F., Lapinte, V., Caillol, S., Habas, J.P., Robin, J.J. *J. Polym. Sci. Pol. Chem.*, 2011, **49**(11), 2434-2444. DOI: 10.1002/pola.24674.

[4] Hoyle, C.E., Bowman, C.N. *Angew. Chem. Int. Ed.*, 2010, **49**(9), 1540-1573. DOI: 10.1002/anie.200903924.

[5] Ionescu, M., Radojčić, D., Wan, X., Petrović, Z.S., Upshaw, T. A. *Eur. Polym. J.*, 2015, **67**, 439-448. DOI: 10.1016/j.eurpolymj.2014.12.037.

[6] Hoyle, C.E., Lee, T.Y., Roper, T. *J. Polym. Sci. Pol. Chem.*, 2004, **42**(21), 5301-5338. DOI: 10.1002/pola.20366.

[7] Desroches, M., Caillol, S., Lapinte, V., Auvergne, R., Boutevin, B. *Macromolecules*, 2011, **44**, 2489-2500. DOI: 10.1021/ma102884w.

[8] Zhang, C., Garrison, T.F., Madbouly, S.A., Kessler, M.R. *Prog. Polym. Sci.*, 2017, **71**, 91-143. DOI: 10.1016/j.progpolymsci.2016.12.009.

[9] Türünç, O., Meier, M.A. *Eur. J. Lipid Sci. Tech.*, 2013, **115**(1), 41-54. DOI: 10.1002/ejlt.201200148.

[10] Guo, A., Demydov, D., Zhang, W., Petrovic, Z.S. *J. Polym. Environ.*, 2002, **10**(1), 49-52. DOI: 10.1023/A:1021022123733.

[11] Petrović, Z.S., Guo, A., Javni, I., Cvetković, I., Hong, D.P. *Polym. Int.*, 2008, **57**(2), 275-281. DOI: 10.1002/pi.2340.

[12] Desroches, M., Escouvois, M., Auvergne, R., Caillol, S., Boutevin, B*Polym. Rev.*, 2012, **52**(1), 38-79. DOI: 10.1080/15583724.2011.640443.

[13] Ghasemlou, M., Daver, F., Ivanova, E.P., Adhikari, B. *Ind. Crops Prod.*, 2019, **142**, 111841. DOI: 10.1016/j.indcrop.2019.111841.

[14] Mazo, P.C., Rios, L.A. *Chem. Eng. J.*, 2012, **210**, 333-338. DOI: 10.1016/j.cej.2012.08.099.

[15] Mazo, P., Rios, L. *J. Am. Oil Chem. Soc.*, 2013, **90**(5), 725-730. DOI: 10.1007/s11746-013-2214-3.

[16] Guzmán, A. F., Echeverri, D.A., Rios, L. A. *J. Chem. Technol. Biotech.*, 2017, **92**(5), 1104-1110. DOI: 10.1002/jctb.5104.

[17] Palaskar, D.V., Boyer, A., Cloutet, E., Le Meins, J.F., Gadenne, B., Alfos, C., Farcet, C., Cramail, H. *J. Polym. Sci. Pol. Chem.*, 2012*,* **50**(9), 1766-1782. DOI: 10.1002/pola.25944.

[18] Zhang, C., Madbouly, S.A., Kessler, M.R*ACS Appl. Mater. Inter.*, 2015, **7**(2), 1226-1233. DOI: 10.1021/am5071333.

[19] Alagi, P., Choi, Y.J., Hong, S.C. *Eur. Polym. J.*, 2016, **78**, 46-60. DOI: 10.1016/j.eurpolymj.2016.03.003.

[20] Alagi, P., Ghorpade, R., Jang, J.H., Patil, C., Jirimali, H., Gite, V., Hong, S.C. *Ind. Crops Prod.*, 2018, **113**, 249-258. DOI: 10.1016/j.indcrop.2018.01.041.

[21] Feng, Y., Liang, H., Yang, Z., Yuan, T., Luo, Y., Li, P., Yang, Z, Zhang, C. *ACS Sustain. Chem. Eng.*, 2017, **5**(8), 7365-7373. DOI: 10.1021/acssuschemeng.7b01672.

[22] Mokhtari, C., Malek, F., Caillol, S., Negrell, C *Eur. J. Lipid Sci. Tech*., 2018, **120**(3), 1700414. DOI: 10.1002/ejlt.201700414.

[23] Mokhtari, C., Malek, F., Halila, S., Belgacem, M.N., Khiari, R *J. Renew. Mater.*, 2021, **9**(7), 1213. DOI: 10.32604/jrm.2021.015475.

[24] Ramanujam, S., Zequine, C., Bhoyate, S., Neria, B., Kahol, P.K., Gupta, R.K. *C*, 2019, **5**(1), 13. DOI: 10.3390/c5010013.

[25] Shen, Y., He, J., Xie, Z., Zhou, X., Fang, C., Zhang, C. *Ind. Crops Prod.*, 2019, **140**, 111711. DOI: 10.1016/j.indcrop.2019.111711.

[26] Mokhtari, C., Malek, F., Manseri, A., Caillol, S., Negrell, C. *Eur. Polym. J.*, 2019, **113**, 18-28. DOI: 10.1016/j.eurpolymj.2019.01.039.

[27] Stemmelen, M., Lapinte, V., Habas, J.P., Robin, J.J. *Eur. Polym. J.,* 2015, **68**, 536-545. DOI: 10.1016/j.eurpolymj.2015.03.062.

[28] Sammaiah, A., Padmaja, K.V., Prasad, R.B. *Eur. J. Lipid Sci. Tech.*, 2016, **118**(3), 495-502. DOI: 10.1002/ejlt.201500119.

[29] Echeverri, D.A., Inciarte, H.C., Cortés, N., Estenoz, D.A., Polo, M.L., Rios, L.A*J. App. Polym. Sci.,* 2023, e54036. DOI: 10.1002/app.54036.

[30] Chatgilialoglu, C., Ferreri, C., Ballestri, M., Mulazzani, Q. G., Landi, L. *J. Am. Chem. Soc.,* 2000, **122**(19), 4593-4601. DOI: 10.1021/ja994169s.

[31] Chatgilialoglu, C., Altieri, A., Fischer, H. *J. Am. Chem. Soc.*, 2002, **124**(43), 12816-12823. DOI: 10.1021/ja027428d.

[32] Chatgilialoglu, C., Samadi, A., Guerra, M., Fischer, H. *ChemPhysChem,* 2005, **6**(2), 286-291. DOI: 10.1002/cphc.200400388.

[33] Chatgilialoglu, C., Ferreri, C., Guerra, M., Samadi, A., Bowry, V.W. *J. Am. Chem. Soc.*, 2017, **139**(13), 4704-4714. DOI: 10.1021/jacs.6b11320.

[34] Chatgilialoglu, C., Bowry, V.W. *J. Org. Chem.*, 2018, **83**(16), 9178-9189. DOI: 10.1021/acs.joc.8b01216.

[35] Ferreri, C., Costantino, C., Perrotta, L., Landi, L., Mulazzani, Q.G., Chatgilialoglu, C. *J. Am. Chem. Soc.*, 2001, **123**(19), 4459-4468. DOI: 10.1021/ja0040969.

[36] Claudino, M., Johansson, M., Jonsson, M. *Eur. Polym. J.*, 2010, **46**(12), 2321-2332. DOI: 10.1016/j.eurpolymj.2010.10.001.

[37] Mengele, E.A., Ferreri, C., Chatgilialoglu, C., Kasaikina, O.T. *Mosc. Univ. Chem. Bull.*, 2010, **65**(3), 210-211. DOI: 10.3103/S002713141003020X.

[38] Mengele, E.A., Krugovov, D.A., Kasaikina, O.T. *Russ. Chem. Bull.*, 2015, **64**(4), 846-851. DOI: 10.1007/s11172-015-0943-1.

[39] Mihaljević, B., Tartaro, I., Ferreri, C., Chatgilialoglu, C. *Org. Biomol. Chem.*, 2011, **9**(9), 3541-3548. DOI: 10.1039/C1OB05083D.

[40] Biermann, U., Butte, W., Koch, R., Fokou, P.A., Türünç, O., Meier, M.A., Metzger, J.O. *Chem. Eur. J.*, 2012, **18**(26), 8201-8207. DOI: 10.1002/chem.201103252.

[41] Bujak, IT., Chatgilialoglu, C., Ferreri, C., Valgimigli, L., Amorati, R., Mihaljević, B. *Radiat. Phys. Chem.*, 2016, **124**, 104-110. DOI: 10.1016/j.radphyschem.2015.11.018.

[42] Zhao, Y.H., Hupin, S., Lecamp, L., Vuluga, D., Afonso, C., Burel, F., Loutelier-Bourhis, C. *RSC Adv.*, 2017, **7**(6), 3343-3352. DOI: 10.1039/C6RA25633C.

[43] González-Paz, R., Cádiz, V., Kiara, R., Vega-Baudrit, J*J. Nanosci. Nanotechno.*, 2017, **17**(8), 5436-5444. DOI: 10.1166/jnn.2017.13791.

[44] Mucci, V., Vallo, C. *J. App. Polym Sci.*, 2012, **123**(1), 418-425. DOI: 10.1002/app.34473.

[45] Fischer, H., Baer, R., Hany, R., Verhoolen, I., Walbiner, M. *J. Chem. Soc., Perkin Trans. 2,* 1990, **2**(5), 787-798. DOI: 10.1039/C8RE00171E.

[46] Degirmenci, I. *J. Turk. Chem. Soc. A: Chem.*, 2022, **9**(1), 149-162. DOI: 10.18596/jotcsa.1003469.

[47] Frankel, E.N. Hidroperoxide formation. In *Lipid Oxidation*, 2nd ed.; Oily Press Lipid Library Series, Vol. 18 Woodhead Publishing Limited, 2012; 25-50. DOI: 10.1533/9780857097927.25.

[48] Cramer, N.B., Davies, T., O'Brien, A.K., Bowman, C.N. *Macromolecules*, 2003, **36**(12), 4631-4636. DOI: 10.1021/ma034072x.

[49] Ferreri, C., Samadi, A., Sassatelli, F., Landi, L., Chatgilialoglu, C. *J. Am. Chem. Soc.*, 2004, **126**(4), 1063-1072. DOI: 10.1021/ja038072o.

[50] González-Paz, R. J., Lluch, C., Lligadas, G., Ronda, J.C., Galià, M., Cádiz, V. *J. Polym. Sci. Pol. Chem.*, 2011, **49**(11), 2407-2416. DOI: 10.1002/pola.24671.

[51] Sprinz, H., Schwinn, J., Naumov, S., Brede, O. *BBA-MOL CELL BIOL L*, 2000, **1483**(1), 91-100. DOI: 10.1016/S1388-1981(99)00175-4.

Table of Contents (TOC) Image